

END-PUMPED MONOBLOCK LASER FOR EYESAFE TARGETING SYSTEMS

Bradley W. Schilling*, Stephen Chinn, A. D. Hays, Lew Goldberg, C. Ward Trussell
US ARMY RDECOM CERDEC
Night Vision and Electronic Sensors Directorate (NVESD)
Ft. Belvoir, VA 22060

ABSTRACT

We describe a next-generation monoblock laser capable of greater than 10 mJ, 1.5 μm output at 10 pulses per second (PPS) over broad ambient temperature extremes with no active temperature control. The transmitter design is based on a Nd:YAG laser with a Cr^{4+} passive Q-switch and intracavity KTP OPO. In order to achieve the repetition rate and efficiency goals of this effort, but still have wide temperature capability, we are end-pumping the Nd:YAG slab with a 12-bar stack of 100 W (each) diode bars. We compare different techniques for focusing the pump radiation into the 4.25 mm x 4.25 mm end of the slab, including a lensed design, a reflective concentrator, and a lens-duct. We demonstrate wide-temperature operation (-20 to 50 degrees Celsius) for each end-pumped configuration.

1.0 INTRODUCTION

Laser technology to reduce the cost, size, and weight of laser-based military systems is critical to the Army's highly mobile force. Laser targeting applications for Army Future Combat System (FCS) and Future Force Warrior (FFW) include eyesafe laser rangefinding, laser illumination for gated 2D imaging and 3D laser radar systems. These systems require high peak-power laser sources in the eyesafe wavelength band, with pulse energies near 10 mJ, and pulse durations less than 20 ns. Central to this class of laser we continue to develop an enabling technology coined the "monoblock laser" due to its one-piece nature and simplicity of manufacture (Nettleton, 2000). Variations of this laser have been used in several prototype and limited production systems, including the STORM multi-function laser system, and as an illumination laser for a short wave infrared (SWIR) gated-imaging system (Vollmerhausen, 2003). Recently, we have been experimenting with technology to improve the repetition-rate and efficiency of the monoblock laser. Improvements in these parameters directly effect the speed at which FCS/FFW targeting operations can occur and system power consumption (which equates to battery life for many hand-held systems), respectively.

The first generation monoblock laser assemblies employ a flashlamp-pumped architecture based on cost considerations, the robust and mature nature of the technology, and its ability to function well over a broad range of temperatures. However, flashlamps are very broadband sources, producing radiation over many hundreds of nanometers (nm) from the UV to infrared wavelengths. As Figure 2 shows, the targeted absorption of Nd:YAG is strongest in narrow bands between 790 nm and 825 nm. The majority of emitted flashlamp energy, therefore, does not contribute to population inversion in the gain material, but generates unwanted heat, reducing the laser's repetition rate capability and efficiency. A common alternative to lamp-pumped solid state lasers is to optically pump the gain material directly with semiconductor diode lasers. As the dotted trace in Figure 2 shows, a typical pump-diode operates with a comparatively narrow optical bandwidth. Diode-pump sources are selected that overlap the absorption region of the gain material, virtually eliminating out-of-band pump radiation that produces heat. Unfortunately, there is a drawback to diode-pumping solid-state lasers: the diode wavelength changes significantly with temperature. Over a 70 degree Celsius (C) temperature span, the center wavelength will shift by as much as 30 nm. In practice, pump-diodes are often temperature controlled to ensure that the diode wavelength remains on an absorption peak of the gain medium as the ambient temperature drifts or the diodes heat up. Devices used to control diode temperature, such as TE coolers, add system complexity, can be costly and consume relatively large amounts of power. For these reasons, it is desirable to develop diode-pumped solid-state lasers without active temperature control for applications where size, weight, and power consumption are important, such as military-qualified laser systems. Due to the limited absorption length inherent in side-pumped configurations, these designs are particularly susceptible to these shifting wavelength issues. The difficulties encountered with side-diode-pumped laser operation over large temperature extremes are discussed and demonstrated experimentally in this paper.

More consistent output over temperature extremes can be obtained with an end-pumped configuration due to its longer absorption length, if the

Report Documentation Page				Form Approved OMB No. 0704-0188	
Public reporting burden for the collection of information is estimated to average 1 hour per response, including the time for reviewing instructions, searching existing data sources, gathering and maintaining the data needed, and completing and reviewing the collection of information. Send comments regarding this burden estimate or any other aspect of this collection of information, including suggestions for reducing this burden, to Washington Headquarters Services, Directorate for Information Operations and Reports, 1215 Jefferson Davis Highway, Suite 1204, Arlington VA 22202-4302. Respondents should be aware that notwithstanding any other provision of law, no person shall be subject to a penalty for failing to comply with a collection of information if it does not display a currently valid OMB control number.					
1. REPORT DATE 01 NOV 2006		2. REPORT TYPE N/A		3. DATES COVERED -	
4. TITLE AND SUBTITLE End-Pumped Monoblock Laser For Eyesafe Targeting Systems				5a. CONTRACT NUMBER	
				5b. GRANT NUMBER	
				5c. PROGRAM ELEMENT NUMBER	
6. AUTHOR(S)				5d. PROJECT NUMBER	
				5e. TASK NUMBER	
				5f. WORK UNIT NUMBER	
7. PERFORMING ORGANIZATION NAME(S) AND ADDRESS(ES) US ARMY RDECOM CERDEC Night Vision and Electronic Sensors Directorate (NVESD) Ft. Belvoir, VA 22060				8. PERFORMING ORGANIZATION REPORT NUMBER	
9. SPONSORING/MONITORING AGENCY NAME(S) AND ADDRESS(ES)				10. SPONSOR/MONITOR'S ACRONYM(S)	
				11. SPONSOR/MONITOR'S REPORT NUMBER(S)	
12. DISTRIBUTION/AVAILABILITY STATEMENT Approved for public release, distribution unlimited					
13. SUPPLEMENTARY NOTES See also ADM002075., The original document contains color images.					
14. ABSTRACT					
15. SUBJECT TERMS					
16. SECURITY CLASSIFICATION OF:			17. LIMITATION OF ABSTRACT UU	18. NUMBER OF PAGES 29	19a. NAME OF RESPONSIBLE PERSON
a. REPORT unclassified	b. ABSTRACT unclassified	c. THIS PAGE unclassified			

difficulties associated with efficient optical coupling can be overcome. Numerous end-pumping techniques have been reported in the literature, including the use of traditional lenses, (Shannon 1991, Verdún 1992, Turi 1995, Snyder 1991) reflective devices, (Liao 1997, Clarkson 1996) lens ducts, (Beach 1996, Fu 1998) 11-13 and other coupling devices.¹⁴ After a thorough survey of these techniques, we selected a few candidates for further testing based on their suitability for pumping the monoblock laser, including the expected impact on overall size, ruggedness, manufacturability, and cost of a laser system. We decided to experiment with end-pumping designs based on microlenses and lens ducts due to the expected high efficiency, (Beach 1996) and with reflective concentrators based on their simplicity. Each end-pumping configuration is described in detail, and its performance measured over temperatures from -20°C to 50°C.

2. LASER DESIGN

2.1 Diode pumping over temperature

Claims concerning the advantages of end-pumping solid-state lasers are numerous, including better extraction efficiency, (Moulton, 1991) better mode quality, (Fu 1998) and improved frequency stabilization (Zhou, 1985). Our primary interest in end-pumping the monoblock laser is the advantage in performance over wide temperature extremes. An important issue for military-qualified diode-pumped laser systems results from the inherent change in diode wavelength with temperature, typically 0.2 – 0.4 nm per °C. This means that over a 70 degree temperature range, the diode wavelength will drift as much as 30 nm. This is an issue because the absorption properties of Nd:YAG have a strong dependence on wavelength. The absorption coefficient, $\alpha(\lambda)$, for 1% doped, bulk Nd:YAG is plotted for a 25 nm span near 800 nm in Figure 1. Pump radiation is absorbed in the laser gain material in accordance with Beer's law: $I(x) = I_0 e^{-\alpha(\lambda)x}$ where I_0 is the initial optical intensity and $I(x)$ is the optical intensity at position x in the gain medium.

Making use of Beer's law and the measured absorption coefficient data for Nd:YAG given in Figure 1, the necessary absorption length to absorb 60%, 70%, 80%, and 90% of the pump radiation in Nd:YAG is shown in Figure 2. From this simple analysis we see that for pump wavelengths near 808 nm, the radiation will be easily absorbed even for very short absorption lengths. On the other hand, as the wavelength of the pump light drifts, due to temperature changes, 30 mm of gain material (or more) may be required to absorb even 60% of the pump light. A dashed line in Figure 2 indicates an absorption length of 8.5 mm, which is the double pass

length available for side pumping a 4.25 mm gain slab. Given the requirement of military qualified lasers to operate over wide temperature extremes, and the need for compact and low-power-consumption laser systems (no active temperature control), we see the advantage that an end-pumped configuration has over side-pumping because of the much longer absorption length. Experimental verification of the problems side-diode-pumped Nd:YAG lasers have over temperature extremes is given in section 3 below.

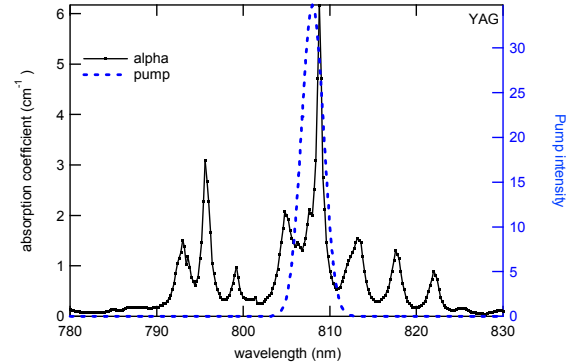


Fig. 1 – Absorption coefficient of 1% doped Nd:YAG vs. wavelength

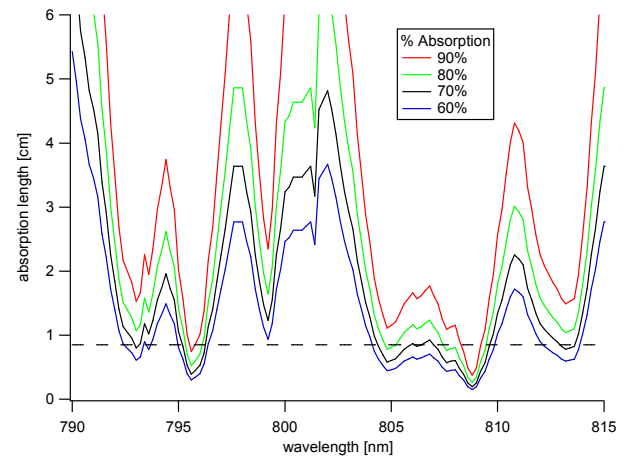


Figure 2 – Beer's Law for Nd:YAG show absorption length required to absorb N% of pump radiation at different wavelengths for N = 60, 70, 80, 90

2.2 Monoblock Laser

A block diagram of the monoblock laser transmitter design is shown in Figure 3 and a photograph of a monoblock laser manufactured by Scientific Materials Corporation (SMC) is shown in Figure 4. The gain medium is a square Nd:YAG laser rod having 1% neodymium doping with a 4.25 mm x 4.25 mm cross-

section that is 30 mm long. The square rod has been cut near the center at Brewster's angle, polished, and mounted in such a way that a slight air gap separates the two Nd:YAG pieces. This configuration encourages oscillation of vertically polarized light while avoiding a deviated cavity due to an optical element positioned at Brewster's angle. The back face of the Nd:YAG crystal is coated to be highly reflective (HR) (>99%) at 1.06 μm and anti-reflective (AR) at the diode wavelength around 808 nm. The second, or output face of the Nd:YAG rod is AR coated at 1.06 μm . The rod is ground on the top and bottom surfaces, and polished on the sides. The polished sides facilitate TIR waveguide confinement of pump radiation in the horizontal plane, while the ground top and bottom help to prevent parasitic oscillations around the slab sides. The Brewster cut in the monoblock laser slab also helps to prevent longitudinal parasitics in the horizontal plane. For the short-pulse operation needed for applications such as rangefinding, and illumination for imaging, the laser employs a Cr⁴⁺-doped YAG (Cr:YAG) passive Q-switch having an unsaturated optical density of 0.27. The Q-switch is AR coated at 1.06 μm on both faces, has a 4.25 mm x 4.25 mm cross section and is about 3 mm long.

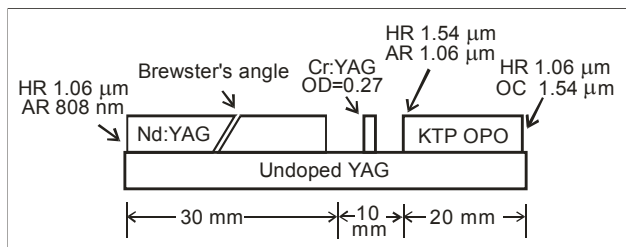


Figure 3 – Diagram of monoblock laser design

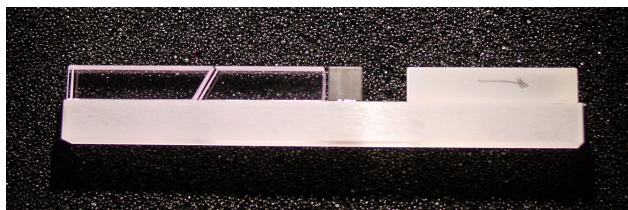


Figure 4 – Monoblock laser

An intracavity OPO configuration is used to shift the laser wavelength from 1.06 μm to 1.54 μm using a monolithic KTP OPO. The input face of the OPO has a dichroic coating, which is AR at 1.06 μm and HR at 1.54 μm . The second face, which acts as the laser output coupler (OC) also has a dichroic coating which is HR at 1.064 μm and 55% reflective at 1.54 μm . All surfaces are flat. When incorporated into the design as shown in Figure 3, the resonator is an intracavity design

in which the 1.06 μm radiation oscillates between the first face of the Nd:YAG crystal and the second face of the KTP OPO. The 1.54 μm radiation oscillates between the parallel faces of the monolithic OPO crystal.

2.3 Pump diode array

Two sets of pump diode bar stacks, manufactured by Coherent Inc., were used for the specific experiments in this paper. These stacks consist of 12 bars generating 100 W/bar, for a total of 1200 W, in Coherent's standard G-stack package. Each bar is about 10 mm in length. The package is designed with 400 μm spacing between diode bars, so the overall area of emission is roughly 4.8 mm (fast axis) x 10 mm (slow axis). The full angle beam divergence for these diode packages are specified at < 35 degrees (fast axis) by 10 degrees (slow axis). For these experiments we used a constant current, constant pulsewidth condition to drive the diodes. Under these constraints, both output energy and wavelength change with temperature. The diode arrays were characterized over the temperature extremes under consideration by recording energy output and wavelength at 2°C increments from -20°C to 50°C. The diode temperature was controlled by pumping heated or chilled fluid through an aluminum heat sink designed for the purpose.

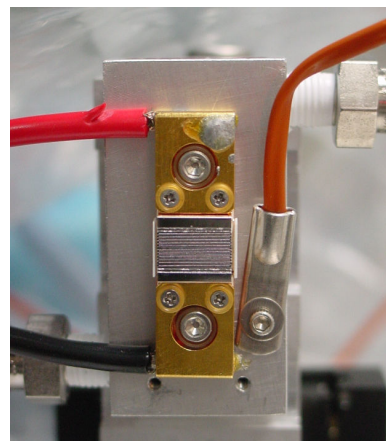


Figure 5 – Photograph of 12-bar pump-diode mounted on aluminum heat sink shows thermocouple location

The diode array package was mounted directly to the heat sink and a thermocouple sensor was mounted in close proximity to the diode, as shown in Figure 5. The measured relationship between wavelength and temperature was very nearly linear with about a 0.25 nm change in wavelength per degree C, as the graph in Figure 6 shows. The wavelength (including both diode stacks), ranged from 794 nm to 812 nm. Figure 7 shows the measured relationships between diode array output energy and temperature, for a constant drive current of 100A and constant drive pulsewidth of 200 μs .

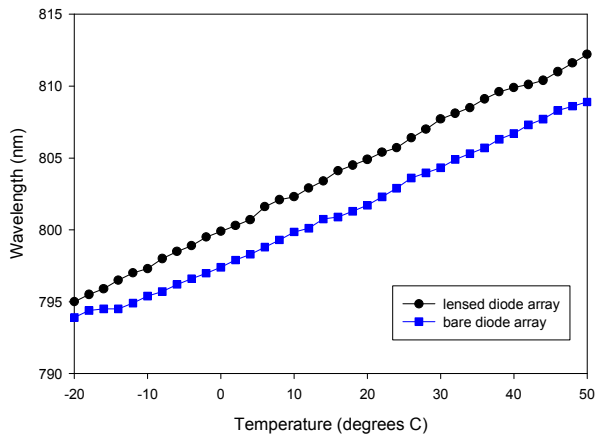


Figure 6 - Pump diode wavelength vs. temperature for two diode arrays. Data taken under constant current (100A) constant pulsewidth (200 μ s) condition.

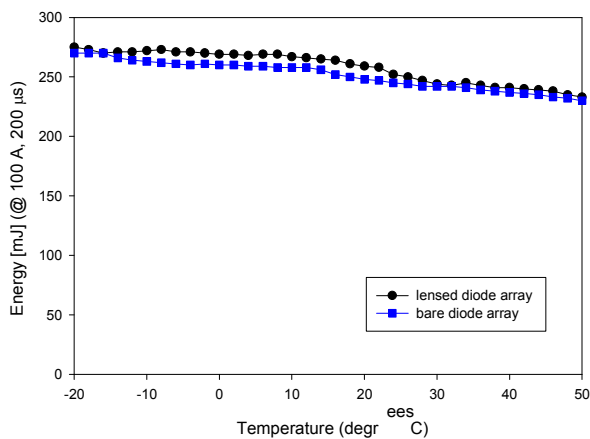


Figure 7 - Pump diode pulse energy vs. temperature for two diode arrays. Data taken under constant current (100A) constant pulsewidth (200 μ s) condition.

3.0 END-PUMPED CONFIGURATIONS

The main difficulty associated with end-pumping solid state lasers with laser-diode stacks is efficiently coupling the pump radiation into the end of the slab. The geometrical mismatch between the effective emitter area and available slab input aperture, in conjunction with the large divergence associated with these semiconductor pump devices, calls for specialized light concentration schemes. We have experimented with several such end-pumping schemes, three of which we report on here. The first configuration uses cylindrical microlenses in the fast axis and a bulk lens in the slow axis to focus the pump radiation into the end of the laser slab. In the second case, a hollow-reflective concentrator was designed to funnel the pump radiation into the resonator.

Finally, a solid YAG lens-duct was fabricated and tested for end-pumping the monoblock laser.

Using a cylinder or rod lens to collimate the 1-cm long bar is quite simple for single bars and even for larger pitch stacks. But when the pitch is small, aligning and attaching the lenses is challenging since each cylinder lens has small diameter, and requires micro-manipulation for precise positioning. Special fixtures and techniques were developed at NVESD to successfully attach fast axis lenses to 12-bar laser diode arrays used to pump the monoblock lasers. GRIN lenses having a 300 μ m diameter from Doric were chosen for this application. Modeling of the emitter indicates the lens must be aligned colinearly with the emitting junction within 2 μ m. Deviations beyond this cause unacceptable steering of the beam. This tolerance must be maintained across the entire bar. Variations across the bar manifest itself as smile in the collimated beam.

Several methods were attempted to hold the long cylinder lenses without success. Any force used to squeeze the end of the lens would bow it. A novel method was developed to hold the ends of the cylinder lens to align it to the laser-diode bar. The tip of a 0.30 mm syringe needle was drilled using a 0.3 mm micro drill bit. The drill bit removed material, but also swelled the tip of the needle slightly to form a socket. The wall thickness in this area is estimated to be less than 20 microns thick. A fixture was used to hold the lens and allow for the needle tips to gently slip over each end. Once held in the alignment fixture it was brought close to the bar to be aligned for parallelism and focus. Adjustments for the arms were setup up such that one was independent and the other moved with the entire assembly. This way once the lens was parallel with the facet the whole assembly was moved to bring the lens into final alignment. The alignment fixture, lens and partially lensed laser-diode array are shown in Figure 8. Once the lens alignment was optimized, as determined by observing the far field distribution of the beam, a small amount of low shrinkage UV curing epoxy was applied to the lens. To maximize the amount of pump radiation entering the laser resonator, the microlenses on the outermost bars are aligned to steer the radiation from these sources slightly toward the optical axis. Subsequently, a single bulk cylindrical lens with focal length $f = 15$ mm is used to focus slow-axis radiation into the end of the laser rod. Once inside of the slab the pump light in the slow axis direction is totally internally reflected by the polished side walls of the slab to insure that the full length of the slab can absorb the light. To measure the efficiency of the lensed configuration, a 4.25 x 4.25 mm aperture, was placed near the focus of the cylindrical lens. The measured optical efficiency of this configuration was about 86%.

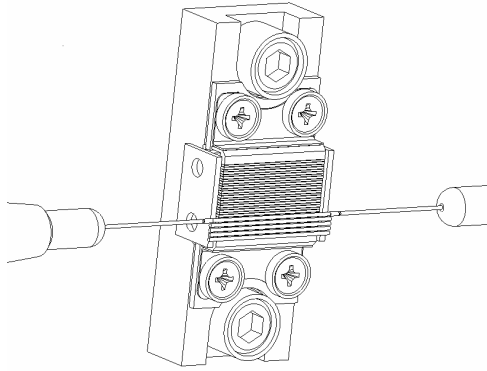


Figure 8 – Drawing of the alignment fixture, lens being aligned and partially lensed laser-diode array

We decided to experiment with the second approach, a hollow-reflective concentrator, due to its simplicity. We fashioned a rectangular “light funnel” from thin (< 1 mm) gold coated mirrors. The launch end of the concentrator is designed to be slightly larger than the diode stack emitting area, approximately 11 mm x 5 mm, while the output end is slightly smaller than the input aperture of the square laser rod, 4.25 mm x 4.25 mm. Determination of the optimum concentrator length involves trading-off small length with concentrator pitch angle. For steep angles the pump light leaves the concentrator with higher divergence, resulting in reduced coupling efficiency. For very steep pitch angles, the radiation can actually reflect back on itself, never leaving the concentrator. Optical ray trace models were used to aid in selecting the optimal concentrator length, of 24 mm. The measured optical efficiency of this reflective concentrator is about 83%.

The third configuration for end-pumping uses a lens duct having the same nominal dimensions as the concentrator discussed above. The lens duct is fabricated from undoped YAG, polished on all sides, and AR coated for the nominal pump wavelength (centered at 808nm) on the entrance and exit surfaces. A lens duct is simple to fabricate and align, like the reflective concentrator, but with better efficiency. When compared to the reflective concentrator, the lens duct is a somewhat more expensive option due to materials cost and optical coating, but is still relatively inexpensive compared to other laser components. The lens duct has a measured optical efficiency of about 90%.

4.0 EXPERIMENTAL RESULTS

To verify the difficulties associated with side-pumping solid-state lasers over large temperature extremes, we arranged the monoblock laser described in section 2.2 in a side-pumped configuration. We used the bare diode array, described in section 2.3 with the output end placed

in close proximity to the side of the gain medium of the monoblock laser. A reflector was placed on the opposite side of the Nd:YAG slab to enable a double-pass absorption path 8.5 mm in length. The diode temperature was taken from -20°C to 50°C , and the $1.5\ \mu\text{m}$ monoblock pulse energy was measured at 2° intervals. The results are plotted in Figure 9, with energy vs. temperature axes on the right and top. As Figure 9 indicates, the laser did not reach threshold for diode temperatures that resulted in pump wavelengths corresponding to low $\alpha(\lambda)$ in Nd:YAG. To emphasize this point, we plotted on the same graph, the percentage of pump radiation that is absorbed in 8.5 mm of bulk Nd:YAG in accordance with Beer’s law, given by: $I(x)/I_0 = e^{-\alpha(\lambda)x}$ for $x = 8.5$ mm. These results indicate that for this case, absorption of somewhere around 80% of the pump light is required to reach the Q-switch threshold. For the side-pumped configuration, this requirement could not be met with 8.5 mm of absorption length for all operating temperatures. This experiment demonstrates why side-pumped schemes are not ideal for military-qualified laser systems that must operate over large temperature bandwidths with size and power constraints that eliminate the possibility of active temperature control.

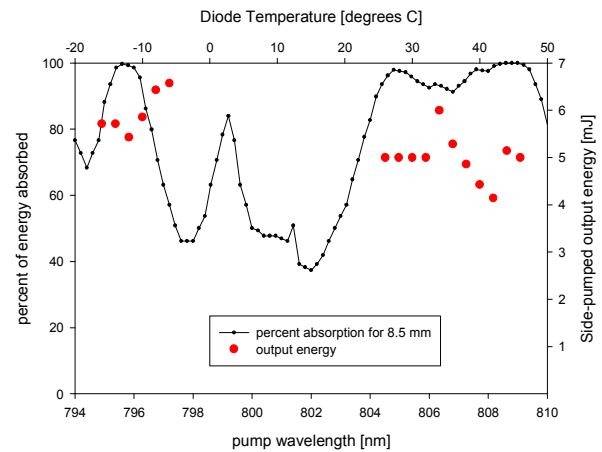


Figure 9 – Output energy vs. temperature (right and top axes) for side pumped configuration along with percent energy absorbed vs. diode wavelength (left and bottom axes) in 8.5 mm of bulk Nd:YAG according to Beer’s law

Next, each of the end-pump configurations described in section 3 was applied to the monoblock laser using the diode stacks characterized in section 2.3. For each end-pumped configuration, the monoblock laser was operated continuously at a 10 Hz repetition rate. The diode temperature was taken from -20°C to 50°C as described above. For every 2°C change in temperature, the Q-switch build-up time and the pulse energy of the $1.5\ \mu\text{m}$ OPO output were recorded. Build-up time was measured with a Tektronix TDS 3054B oscilloscope, and pulse energy was measured with an Ophir PE50

pyroelectric detector. The results are given in Figures 10 and 11.

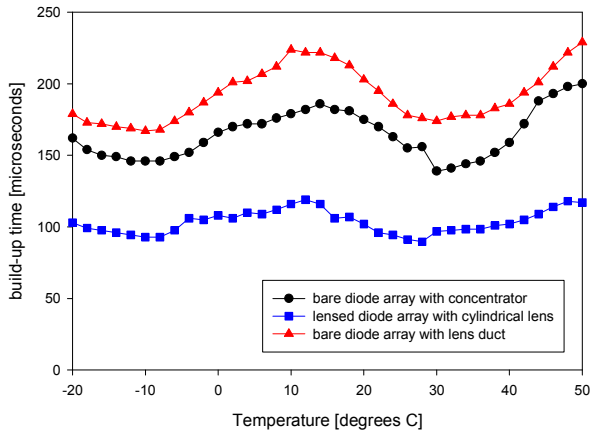


Figure 10 - Build-up time vs. temperature for three end-pumped configurations

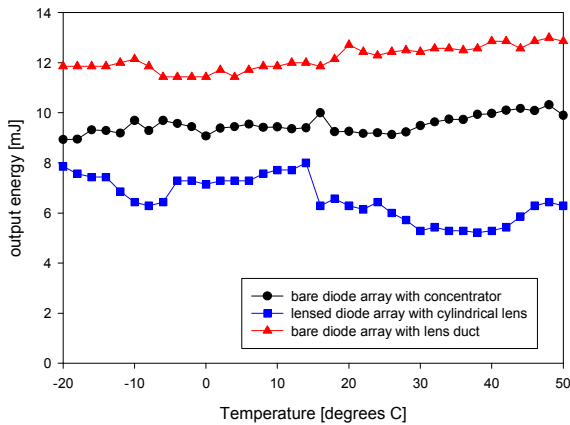


Figure 11 - Output pulse energy vs. temperature for three end-pumped configurations

We also imaged the 1.06 μm fluorescence in the laser gain medium for different pumping and temperature conditions, shown in Figures 12-15. Each of these images show the Nd:YAG rod from the side in a non-lasing condition. Pump times were just less than the time needed to Q-switch. A Cohu 7800 digital camera was used to take the imagery with a 900 nm long-wave-pass filter to block the diode pump light. Care was taken to maintain all camera gain and aperture settings for this data so the comparison would be meaningful. The digital grey-scale images were converted to 8-bit paletted false color images to represent the fluorescence intensity using the color spectrum from white (brightest) to black (dimpest). Figures 12 and 13 show side views of the Nd:YAG laser rod undergoing lensed-diode pumping at temperatures corresponding to maximum absorption and

minimum absorption for the temperature range of interest. Likewise, Figures 14 and 15 show the 1.06 μm fluorescence resulting from end-pumping using the bare diode array with the reflective concentrator for strong and weak absorption. Imagery from the lens duct case was not appreciably different from that of Figures 14 and 15. The images clearly demonstrate the difference in absorption rate for different diode temperatures (wavelengths). At temperatures corresponding to low $\alpha(\lambda)$, the imagery shows that the pump radiation penetrates much more deeply into the gain medium (Figures 12 and 14). Conversely, for large $\alpha(\lambda)$ conditions, the pump radiation is absorbed in a much shorter distance.

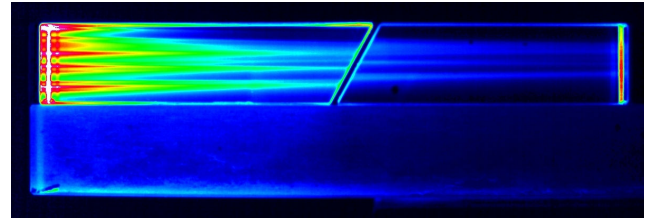


Figure 12 - 1.06 μm fluorescence due to end-pumping with lensed diode array at 12°C

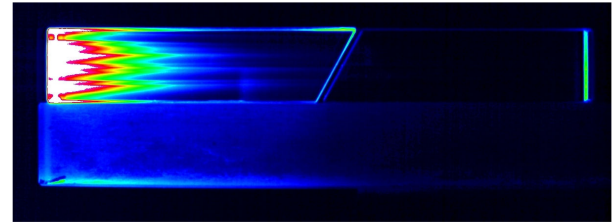


Figure 13 - 1.06 μm fluorescence due to end-pumping with lensed diode array at 30°C

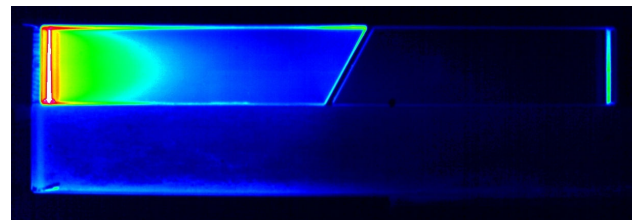


Figure 14 - 1.06 μm fluorescence due to end-pumping with bare diode array at 14°C coupled into Nd:YAG rod by reflective concentrator

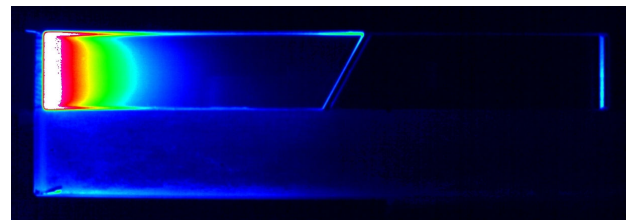


Figure 15 - 1.06 μm fluorescence due to end-pumping with bare diode array at 32°C coupled into Nd:YAG rod by reflective concentrator

5.0 DISCUSSION

As the data shows, each end-pumped configuration operated at a 10 PPS repetition rate over the entire 70°C temperature range with output pulses in the 10 mJ regime. In contrast, when the same laser was side-pumped, lasing only occurred at temperatures corresponding to favorable absorption lengths. From a manufacturing perspective, it was our experience that physically lensing the diode-arrays is difficult, requires special fixturing, and is labor intensive. The concentrator-type devices are easy to align and relatively inexpensive, with the reflective concentrator being the most cost effective. As far as optical throughput is concerned, the lensed configuration and the lens duct have very similar throughput (about 90%), while the reflective device was somewhat less efficient.

From the perspective of 1.5 μm laser output, the lens duct case produced the highest output pulse energy over the entire temperature span, with minimum and maximum pulse energies of 11.4 mJ and 13.0 mJ, respectively. This configuration also had the longest build-up times associated with it, approaching 250 μsec for temperatures associated with weak absorption in the slab. The lensed case operated with consistently shorter build-up times and correspondingly lower output energy, more like 5 to 8 mJ. The reflective concentrator pump configuration, performed somewhere in-between the other two cases.

At first glance, the large variation in output energies for the different configurations is somewhat surprising, given that the same *passively Q-switched* laser is used in each case. We expected to measure relatively consistent output energies for each case, resulting from a consistent level of fluence in the resonator needed to bleach the passive Q-switch, with a difference in buildup times corresponding to the optical efficiencies of each pumping scheme. However, the lensed case consistently produced lower energy pulses, about 50-60% that of the pulse energy for the lens duct. We explain the apparent inconsistency as being due primarily to the spatial characteristics of the pump intensity profile. As the imagery included as Figures 12-15 shows, the pump beam profile for the lensed case has a significant amount of cross-sectional structure, manifested as individual beams radiating down the slab. In contrast, the concentrator seems to homogenize the pump light intensity distribution, making it relatively uniform across the crystal. The highly nonuniform structure in the pump beam is undesirable, particularly for passively Q-switched devices since “hotspots” in the pump profile may lead to localized regions of higher gain and spatially selective bleaching of the Cr:YAG. Such localized bleaching of the Q-switch will result in lower pulse energy since the full cross section of the resonator

may not be contributing to laser action. A correspondingly shorter build-up time is also consistent with local bleaching at hot spots since the Q-switch won't hold-off as long as for the case where pump intensity distribution is uniform. The more uniform pump distribution of the concentrator and lens duct results in larger pulse energies and longer hold-off.

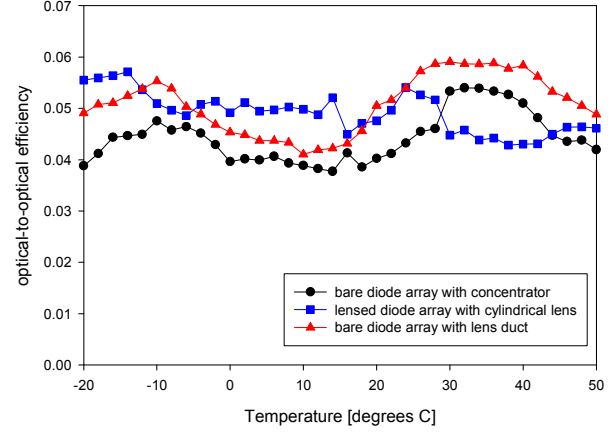


Figure 16 - Optical to optical efficiency vs. temperature for three end-pumped configurations

Finally, we want to investigate the overall optical-to-optical efficiency of the laser, η_o , defined as the ratio of diode-pump energy to 1.5 μm output pulse energy. We calculate the pulse energy needed to achieve Q-switching as:

$$E_p = E_d \left(\frac{\Delta t}{200} \right), \quad (1)$$

where E_p is the pump pulse energy, Δt is the buildup time in μs , and E_d is the measured diode pulse energy for a 200 μs long drive current (given in Figure 7.) Optical efficiency is then given by, $\eta_o = E_o / E_p$, where E_o is the output pulse energy at 1.5 μm . This efficiency, plotted in Figure 16 as a function of temperature, appears to be similar for all pumping configurations, varying between 4% and 6%. Again, the YAG lens duct still has the best overall performance with regard to optical efficiency, but here the reflective concentrator performs the worst, consistent with its low pump throughput efficiency. For comparison we note that the flashlamp-pumped monoblock laser has optical-to-optical efficiency about an order of magnitude lower.

6.0 CONCLUSIONS

In this paper, we address the needs for an eyesafe laser transmitter operating in the 10 millijoule regime at tens

of Hz repetition rate with optical to optical efficiency near 5%. We have described the next generation monoblock laser, a low-cost, compact, and rugged transmitter designed to meet the stringent requirements of military laser systems with application to eyesafe rangefinding and other targeting scenarios. The transmitter design is based on a Nd:YAG laser with a Cr^{4+} passive Q-switch and an intracavity KTP OPO. In order to achieve the repetition rate and efficiency goals of this effort, we experimented with end-pumped versions of the monoblock laser. Our impetus for end-diode-pumping is the improved performance over broad temperature ranges without active heating or cooling. Fundamental to this issue is the change in pump-diode wavelength with temperature and strong wavelength dependence of the absorption coefficient for Nd:YAG. We have shown that the impact of these effects can be mitigated by the long absorption lengths available in end-pumped configurations. We investigated several end-pumping schemes with application to the monoblock laser, each demonstrating higher wall-plug efficiency and repetition rate capability than previous flashlamp-pumped designs. We compared the configurations over a 70°C temperature span from -20°C to 50°C. Each of the tested end-pump configurations gave complete operation over the full temperature range. Although we measured a high pumping efficiency from configuration I, we found the lensed diode array emits a pump beam that contains significant cross-sectional structure. We suspect, based on low overall output energy and short build-up time, this highly structured pump beam leads to partial bleaching of the Q-switch at localized areas of high fluence. We got the best overall performance ($\eta_o = 4\text{--}6\%$) from a pump scheme based on a YAG lens duct, which is easy to manufacture and align. The simple bare diode and concentrator scheme still performed quite well ($\eta_o \sim 4.0\%$) and may have a cost advantage over the lens duct based on material and optical coating considerations. Although not reported on here, we have found that using a lensed diode array in conjunction with a concentrator or lens duct gives a slight improvement over the efficiencies reported here. The funnel-style devices act to homogenize the pump beam while the lensed diodes give the ducts better overall throughput. In our opinion, however, the improvement does not justify the added expense of lensing the diodes for a production-class device.

ACKNOWLEDGMENTS

The authors acknowledge the support received from the Penn State Electro-Optics Center, with special thanks to David Snyder and Jason Carter for lending their technical as well as programmatic expertise to this effort. We would also like to thank John Nettleton and Dallas Barr of NVESD for the many helpful ideas and discussions surrounding the monoblock laser work.

Thanks also to Jeff Leach of NVESD for help with the temperature experiments.

REFERENCES

- Beach, R. J., "Theory and Optimization of lens ducts," Appl. Opt. **35**, 2005-2015 (1996).
- Clarkson, W. A., and Hanna, D. C., "Efficient Nd:YAG laser end pumped by a 20-W diode-laser bar" Opt. Lett. **21**, 869-871 (1996).
- Fu, R. *et al.*, "Design of efficient lens ducts." Appl. Opt. **37**, 4000-4003 (1998).
- Liao, Y. *et al.*, "Highly efficient diode-stack, end-pumped Nd:YAG slab laser with symmetrized beam quality," Appl. Opt. **36**, 20 (1997).
- Moulton, P.F., "Pumping with diodes," IEEE Circuits and Devices Magazine **7**, 36-40 (1991).
- Nettleton, J. E., Schilling, B. W., Barr, D. N. and Lei, J. S., "Monoblock laser for a low-cost, eyesafe, microlaser range finder," Appl. Opt. **39**, 2428-2432, (2000).
- Shannon, D. C. and Wallace, R. W., "High-power Nd:YAG laser end pumped by a cw, 10 mm $3\ 1\ \mu\text{m}$ aperture, 10-W laser-diode bar," Opt. Lett. **16**, 318-320 (1991).
- Snyder, J. J., Reichert, P., and Baer, T. M., "Fast diffraction limited cylindrical microlenses," Appl. Opt. **30**, 2743-2747 (1991).
- Turi, L. and Juhasz, T., "High-power longitudinally end-diode-pumped Nd:YAG regenerative amplifier," Opt. Lett. **20**, 154-156 (1995).
- Verdún, H. R. and Chuang, T., "Efficient TEM₀₀-mode operation of a Nd:YAG laser end pumped by a three-bar high-power diode-laser array," Opt. Lett. **17**, 1000-1002 (1992).
- Vollmerhausen, R. H., Jacobs, E. L., Devitt, N. M., Maurer, T. and Halford, C., "Modeling the target acquisition performance of laser-range-gated imagers," Proc. SPIE Int. Soc. Opt. Eng. 5076, 101 (2003).
- Zhou, B., Kane, T. J., Dixon, G. J., and Byer, B. L., "Efficient, frequency-stable laser-diode-pumped Nd:YAG laser," Opt. Lett. **10**, 62-64 (1985).



END-PUMPED MONOBLOCK LASER FOR EYESAFE TARGETING SYSTEMS

**Bradley W. Schilling, Stephen Chinn, Alan Hays
Lew Goldberg, Ward Trussell**

**US ARMY RDECOM CERDEC
Night Vision and Electronic Sensors Directorate (NVESD)
Ft. Belvoir, VA 22060**

Approved for public release: distribution is unlimited



Overview



- Motivation
 - Laser for targeting applications
 - High peak-power, eyesafe wavelength, high efficiency, high repetition-rate
 - Transition from flashlamp to diode pumping
- Laser Design
- Transition to diode-pumping
 - Nd:YAG absorption characteristics over wavelength
 - Diode characteristics over temperature
 - Optical coupling of pump light
- Laser results over temperature
- Conclusions



Motivation

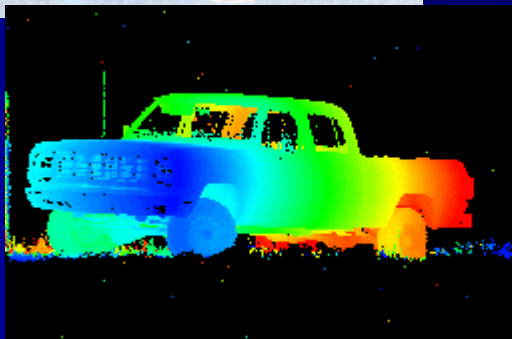
- Laser for targeting applications

- Ranging
- 2D gated SWIR imaging
- 3D flash laser radar



- Required laser source:

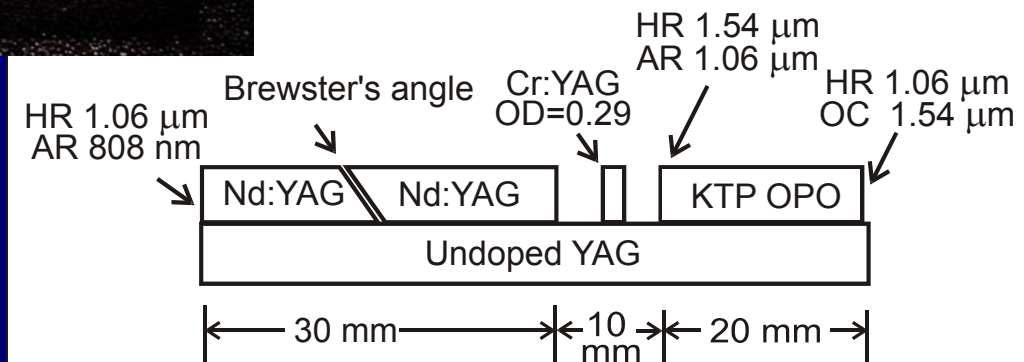
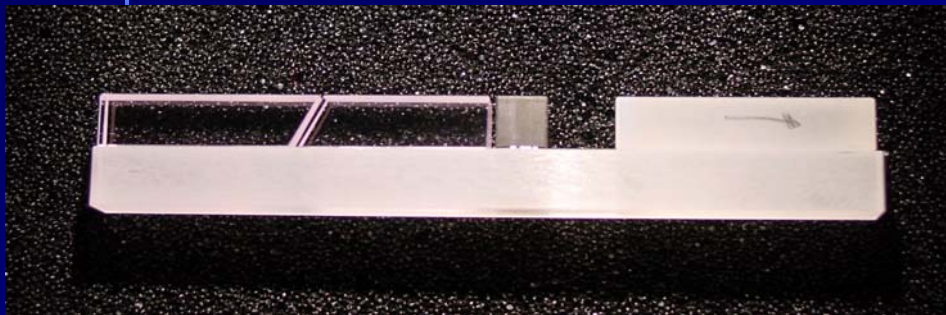
- Energy: $> 10 \text{ mJ}$
- Wavelength: $1.5 \mu\text{m}$ for eyesafety
- Repetition Rate: $> 10 \text{ Hz}$
- High efficiency for battery operation
- Broad ambient temperature operation with no active temperature control.





Monoblock Laser

The transmitter design is based on a Nd:YAG laser with a Cr⁴⁺ passive Q-switch and an intracavity KTP OPO.



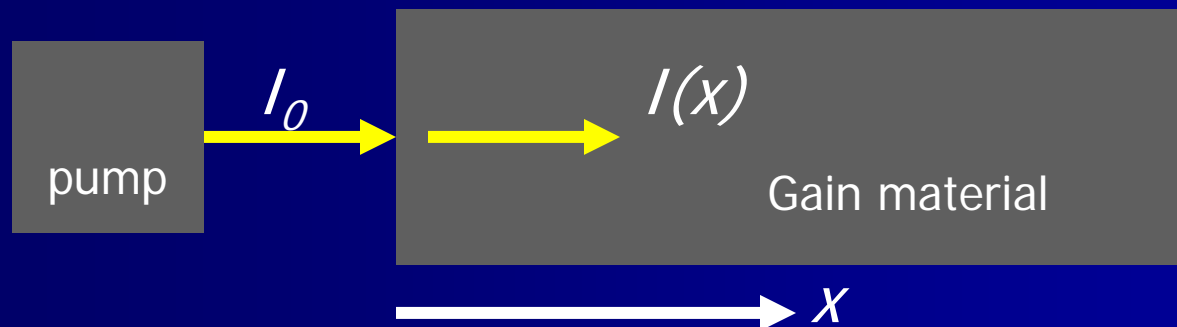
Flashlamp-pumped version in limited production in STORM MFL and in experimental imaging systems (gated SWIR, 3D Ladar)



Optical Pumping

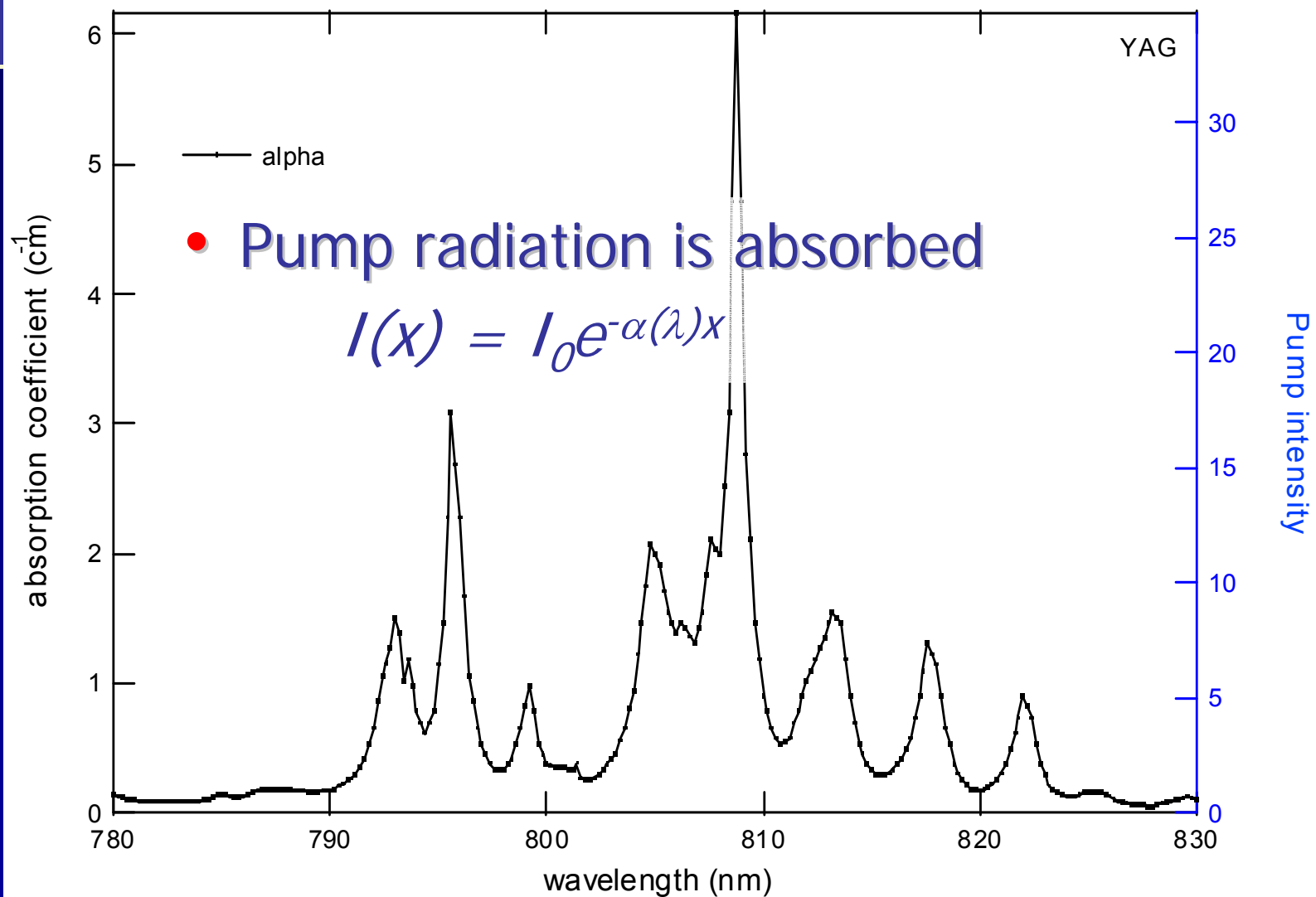
- Monoblock laser is optically pumped
- Photons are absorbed in the gain medium to create a population inversion
- Pump radiation is absorbed

$$I(x) = I_0 e^{-\alpha(\lambda)x}$$



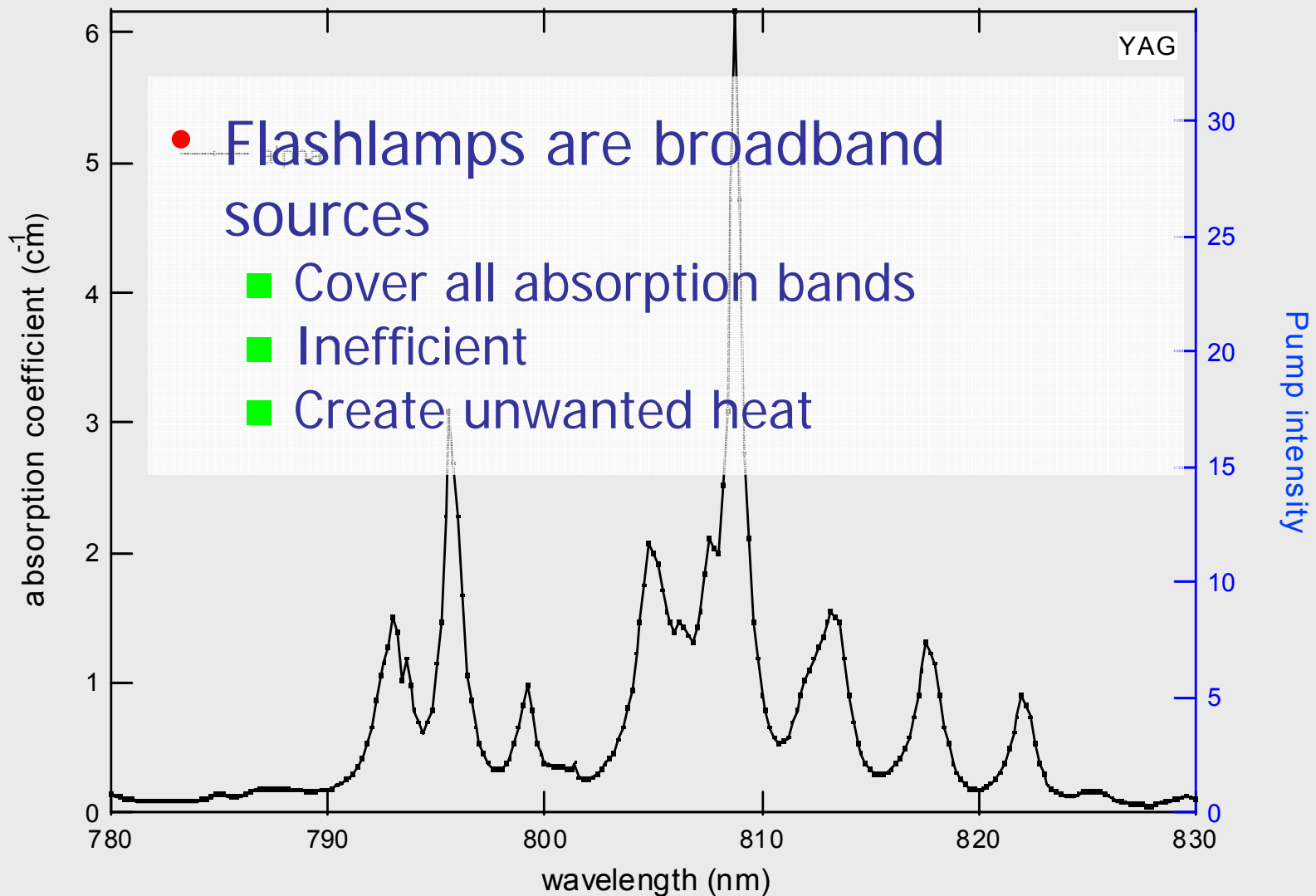


Optical Pumping and Nd:YAG Absorption



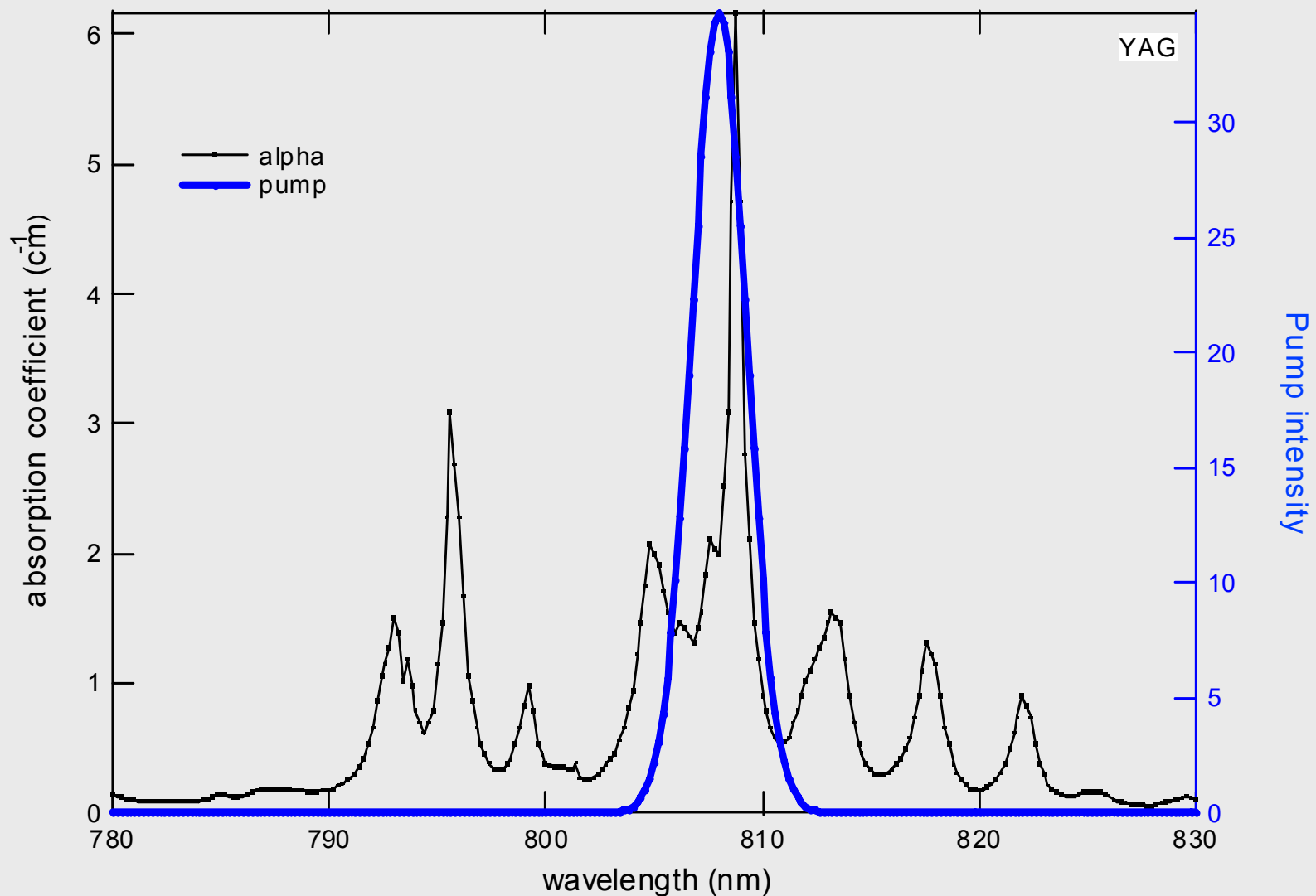


Flashlamp Pumping





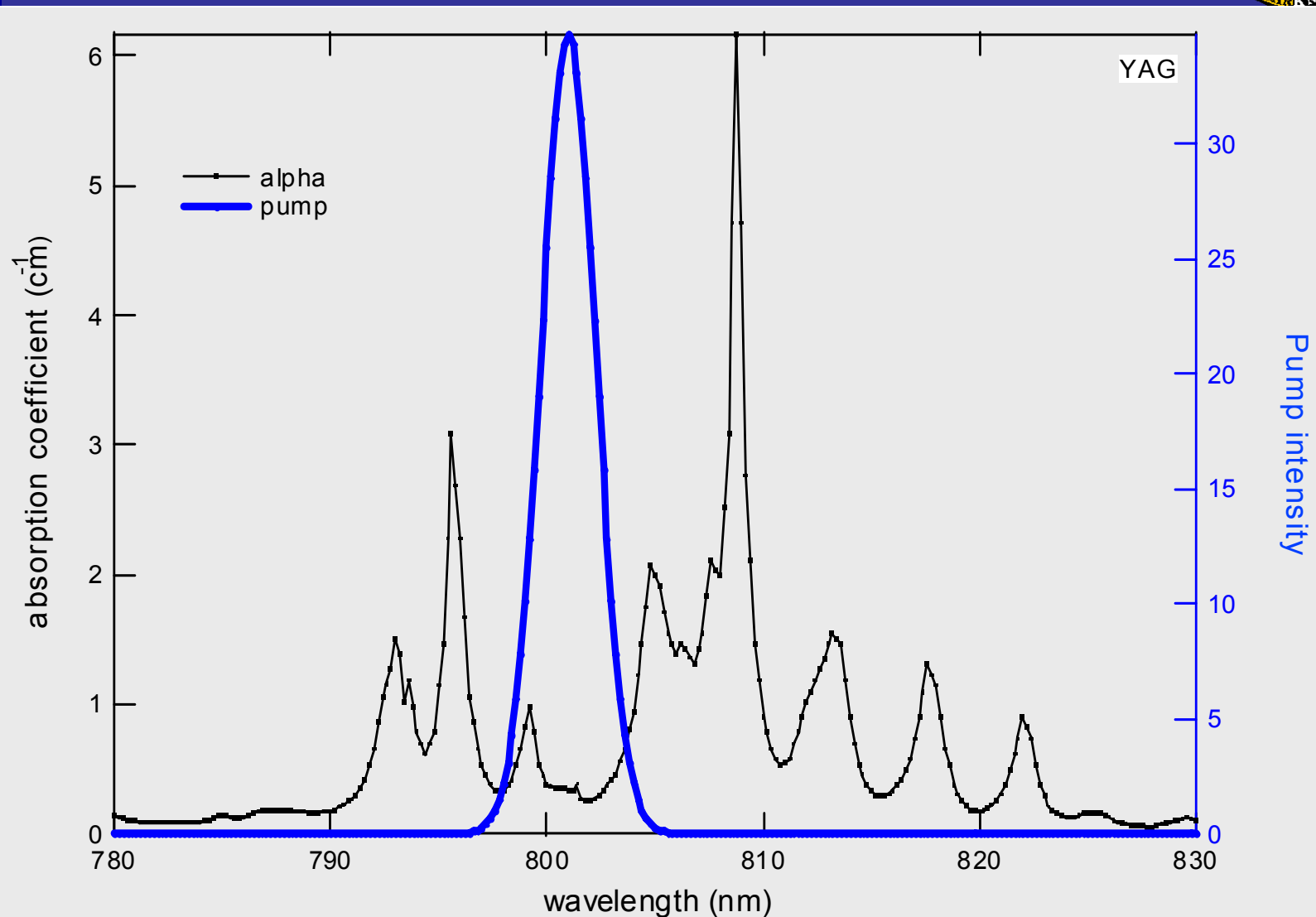
Diode Pumping Nd:YAG



Diode center wavelength 808 nm, 4 nm FWHM



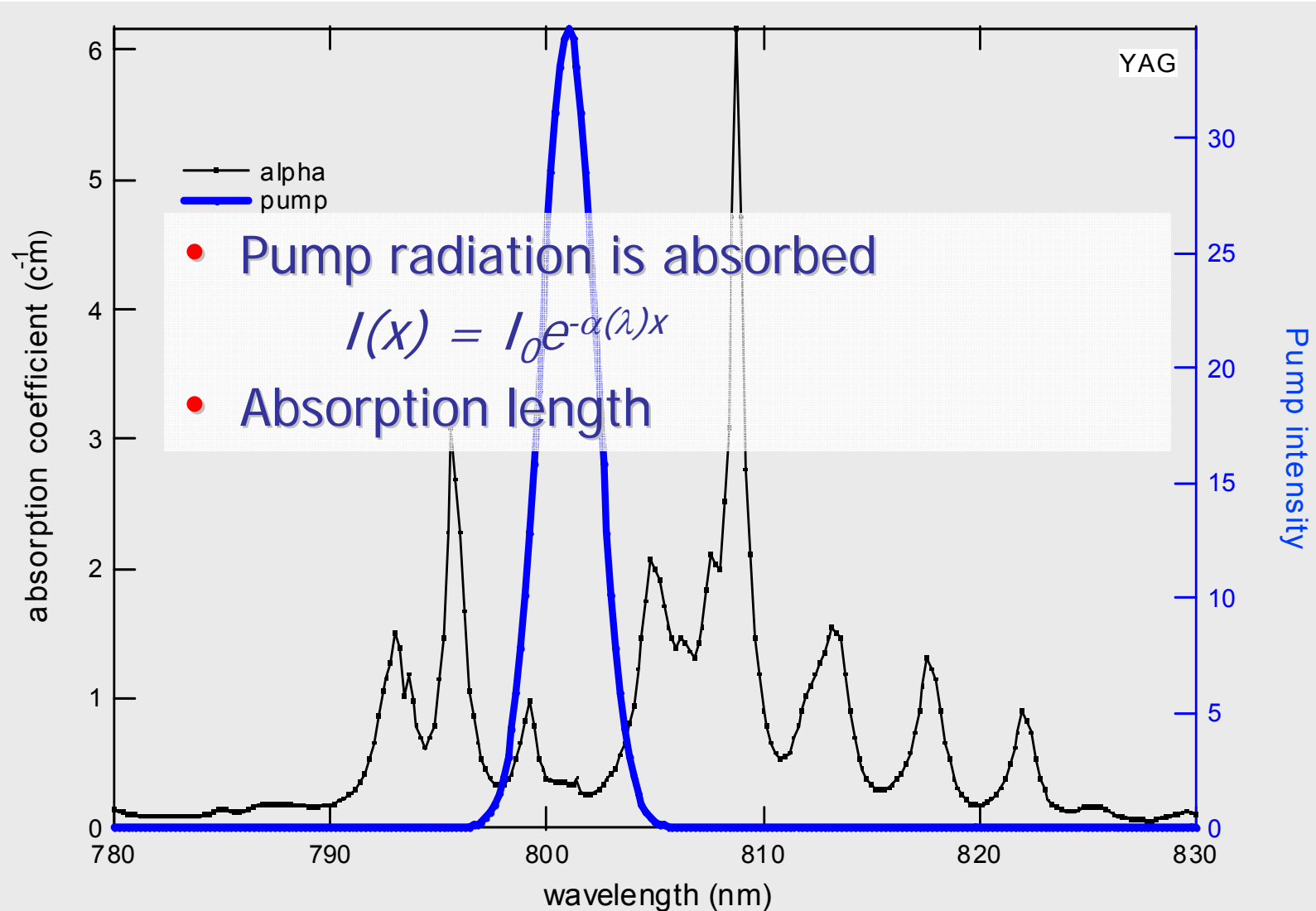
Diode Pumping Nd:YAG



Diode center wavelength 801 nm, 4 nm FWHM



Diode Pumping Nd:YAG

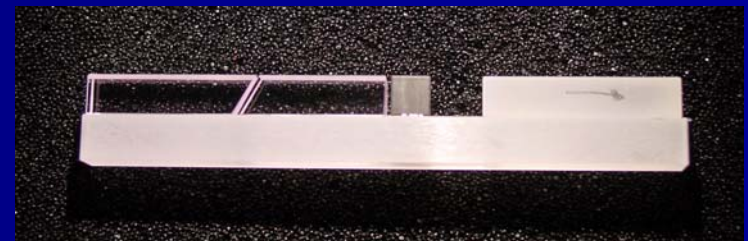
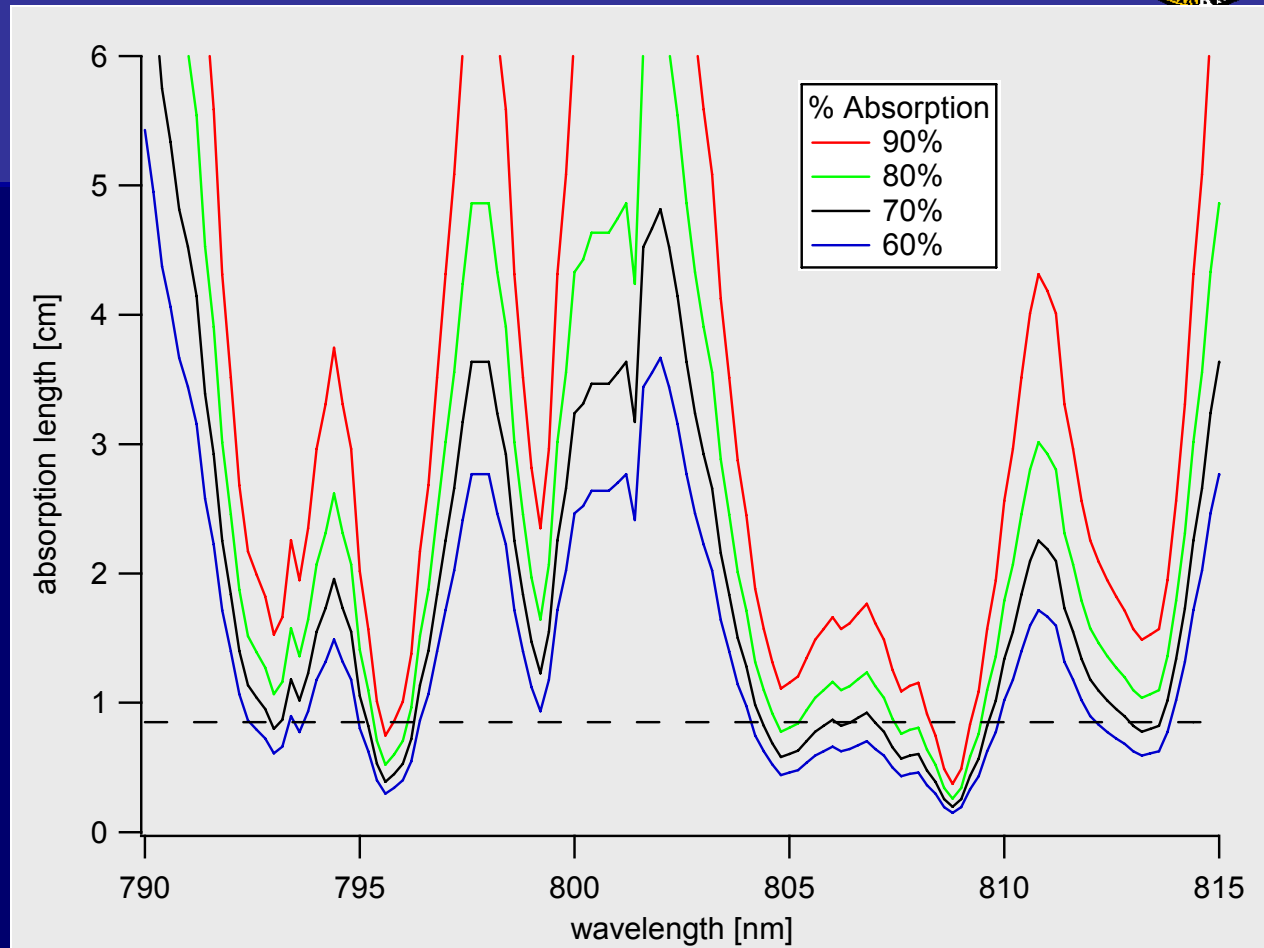


Diode center wavelength 801 nm, 4 nm FWHM



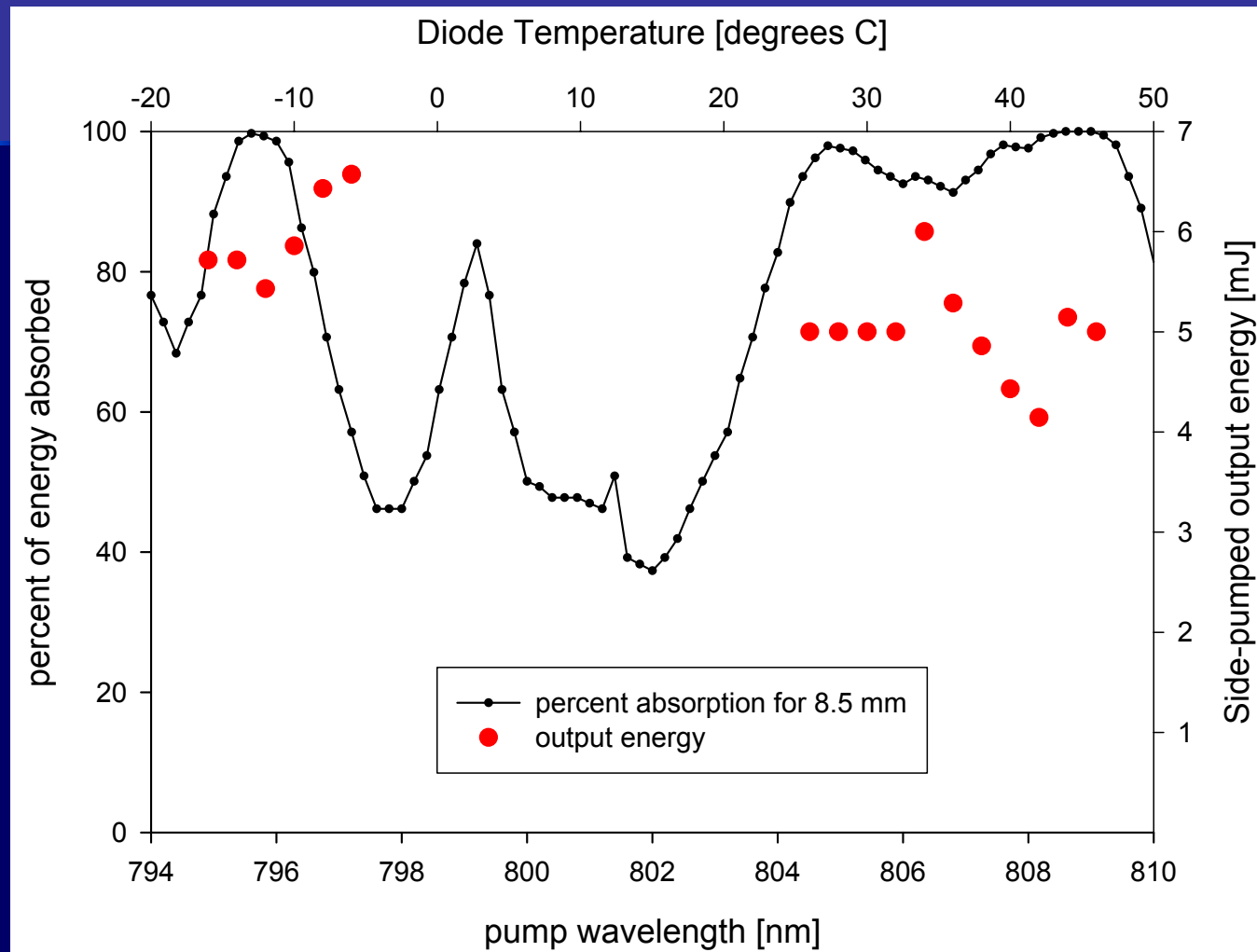
Absorption length vs. Wavelength

Beer's Law
for Nd:YAG
shows
absorption
length
required to
absorb N% of
pump
radiation for
N = 60, 70,
80, 90





Side-pumped Monoblock

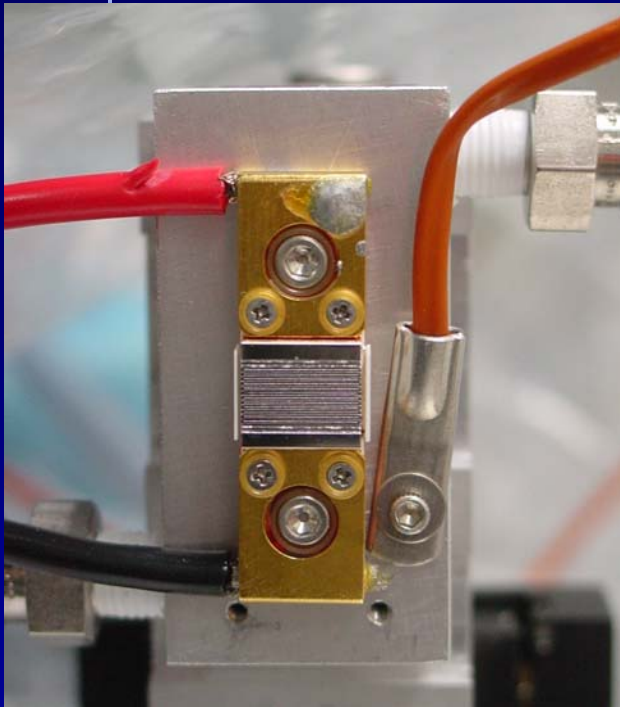


1.5 μm output only at temperatures corresponding to favorable absorption

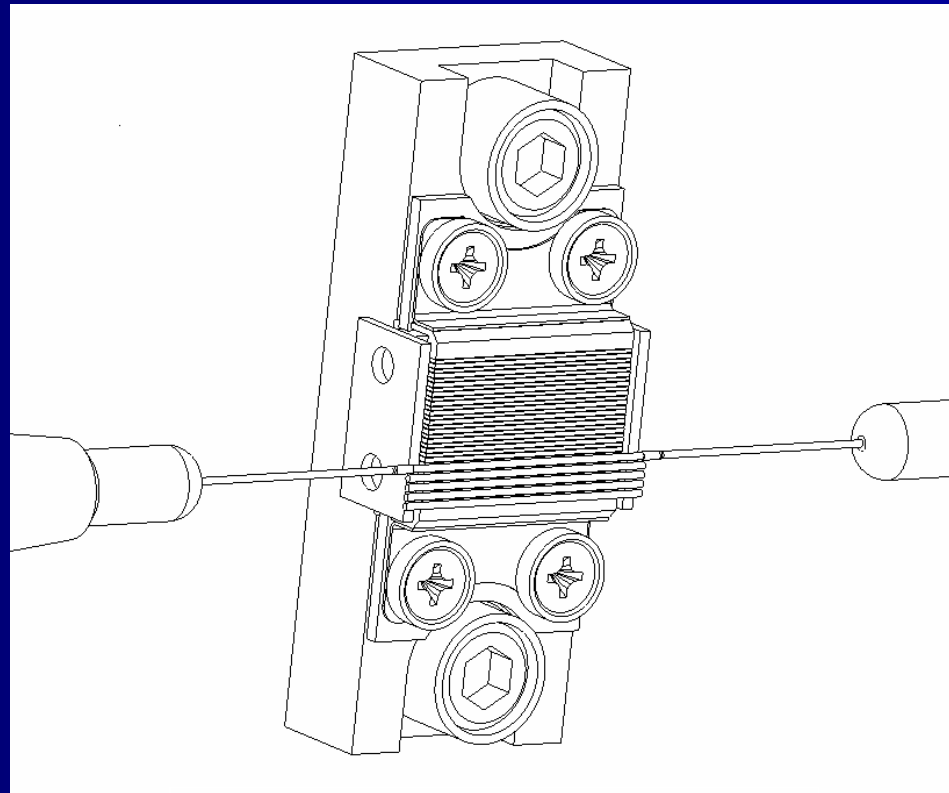


Diode Array

These arrays consist of 12 bar stacks of nominally 100 W/bar diode bars, for a total of 1200 W, in Coherent's standard G-stack package.



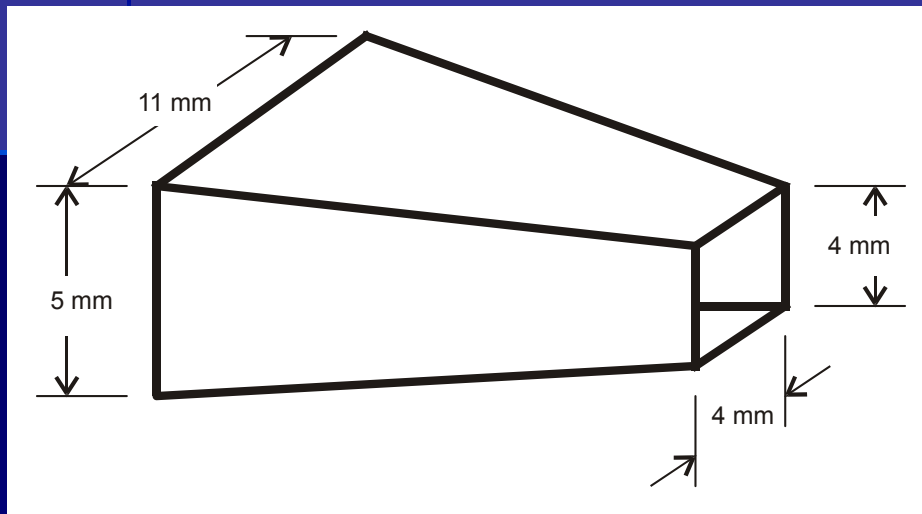
12-bar pump-diode mounted on aluminum heat sink shows thermocouple location



Drawing of the alignment fixture, lens being aligned and partially lensed laser-diode array

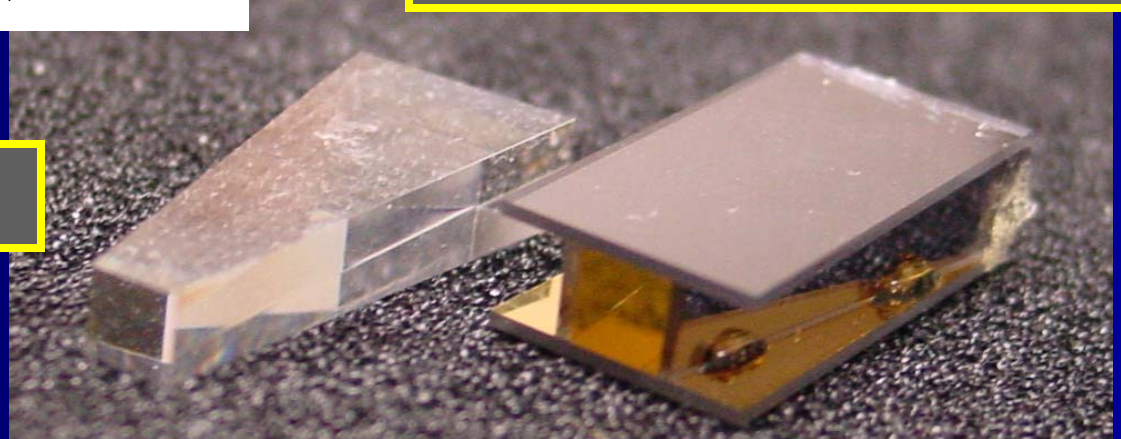


End-Pumping Techniques



Reflective concentrator

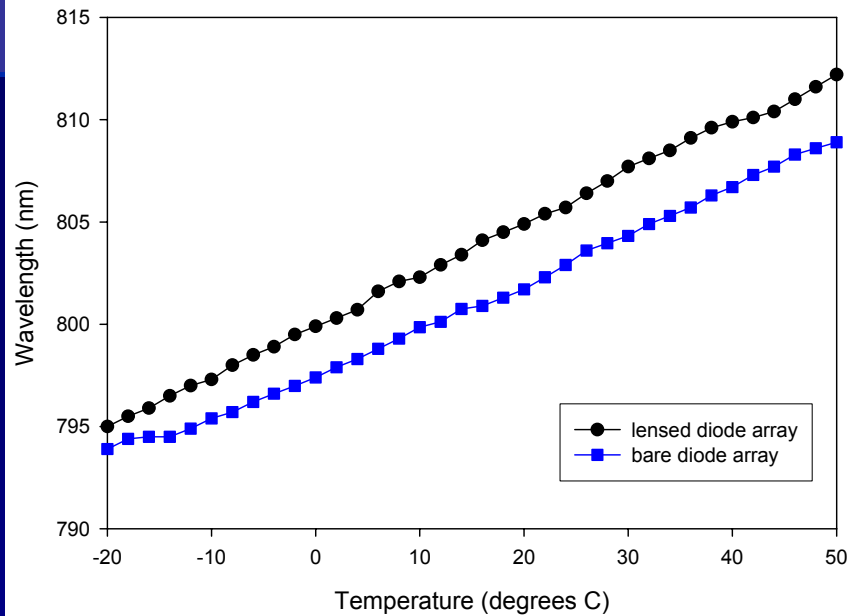
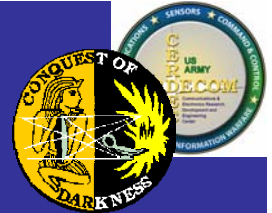
Lens duct



Non-imaging techniques for light concentration

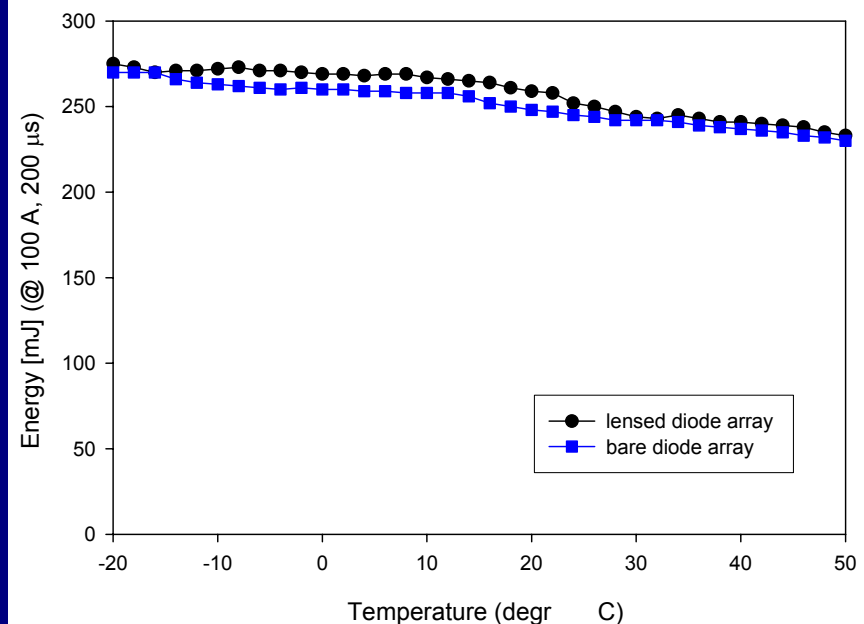


Diode Characterization



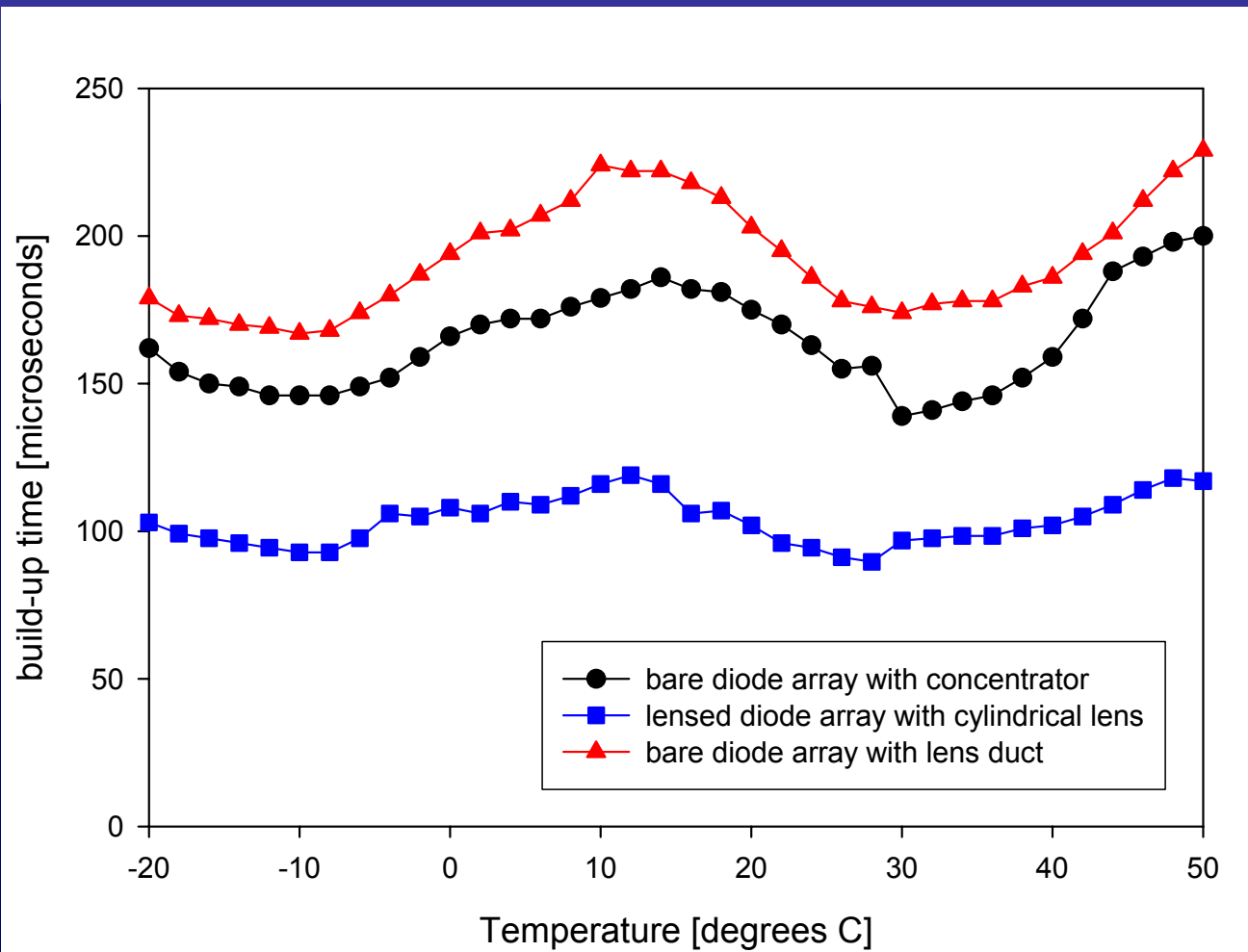
Pump diode wavelength vs. temperature for two diode arrays. Data taken under constant current (100A) constant pulsewidth (200 μ s) condition.

Pump diode pulse energy vs. temperature for two diode arrays. Data taken under constant current (100A) constant pulsewidth (200 μ s) condition.





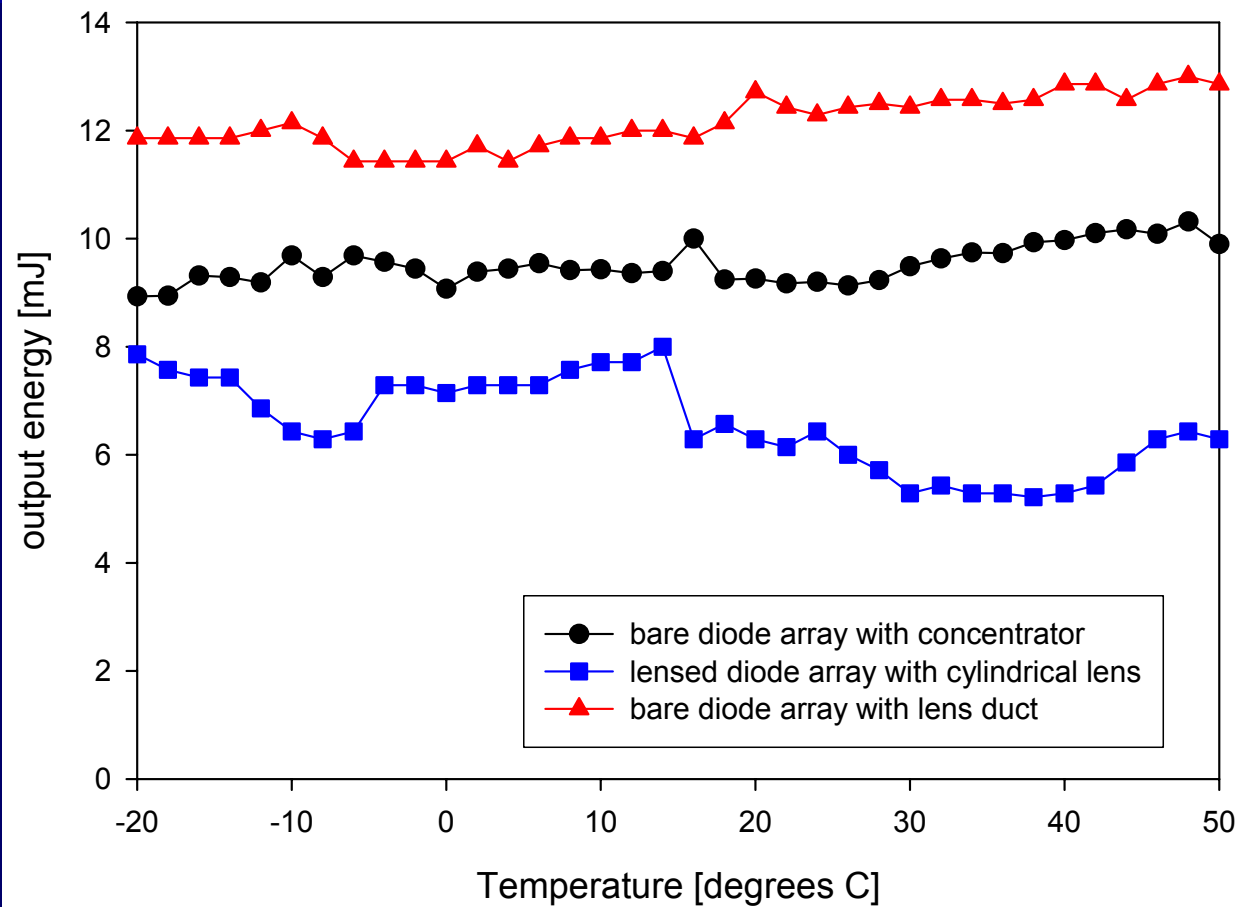
Temperature Testing Build-up Time





Temperature Testing

1.5 μm Energy

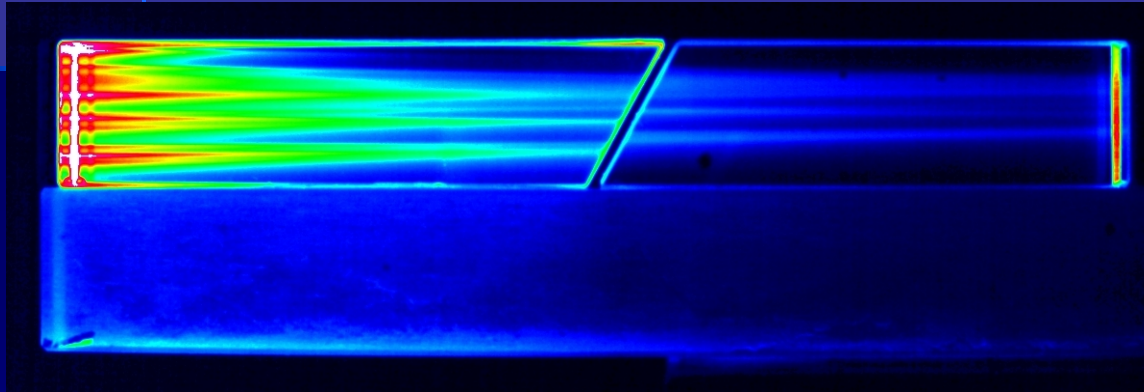




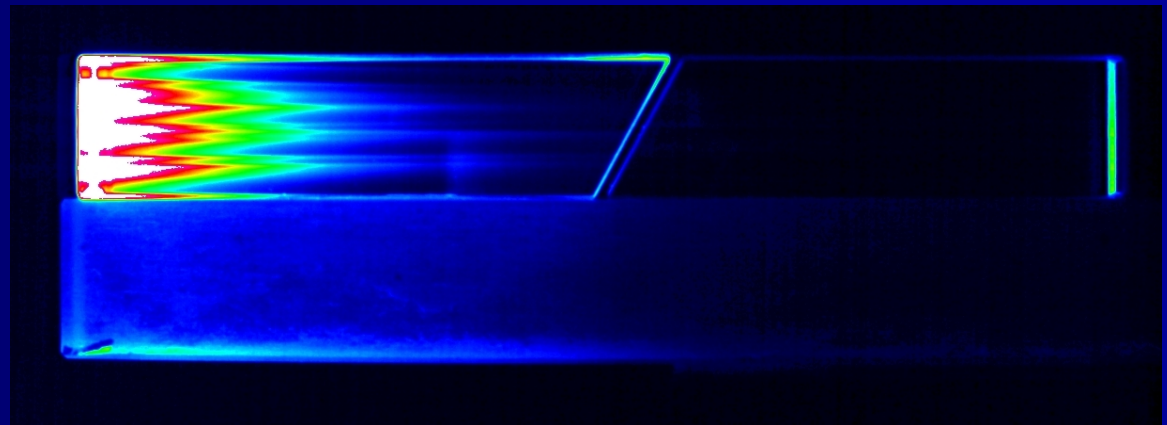
1.06 μm Fluorescence Lensed Case



1.06 μm fluorescence
due to end-pumping
with lensed diode array
at 12°C



1.06 μm fluorescence
due to end-pumping
with lensed diode array
at 30°C



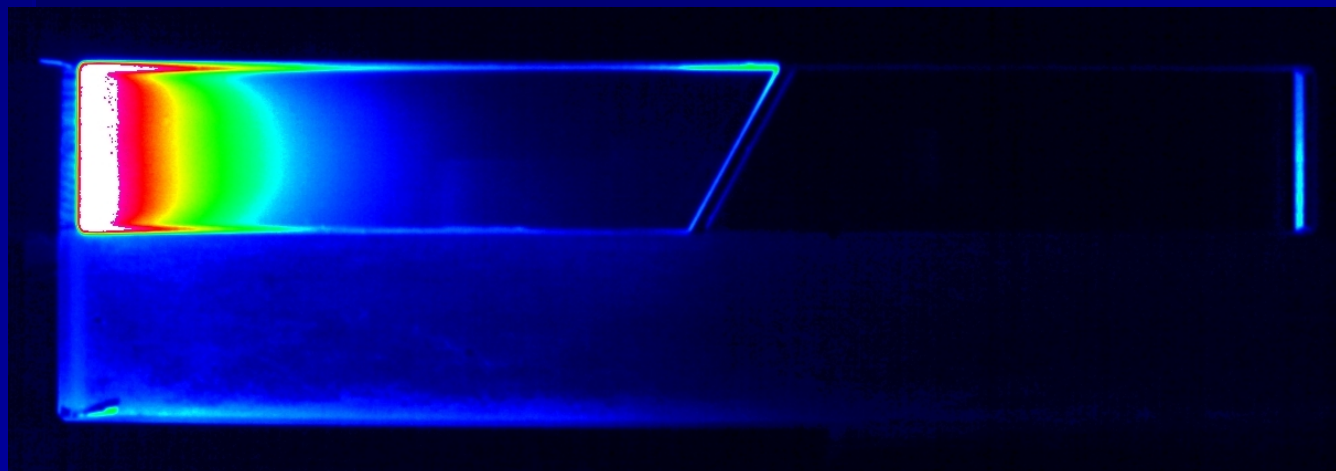


1.06 μm Fluorescence Concentrator Case



14°C

1.06 μm fluorescence due to end-pumping with bare diode array
coupled into Nd:YAG rod by reflective concentrator

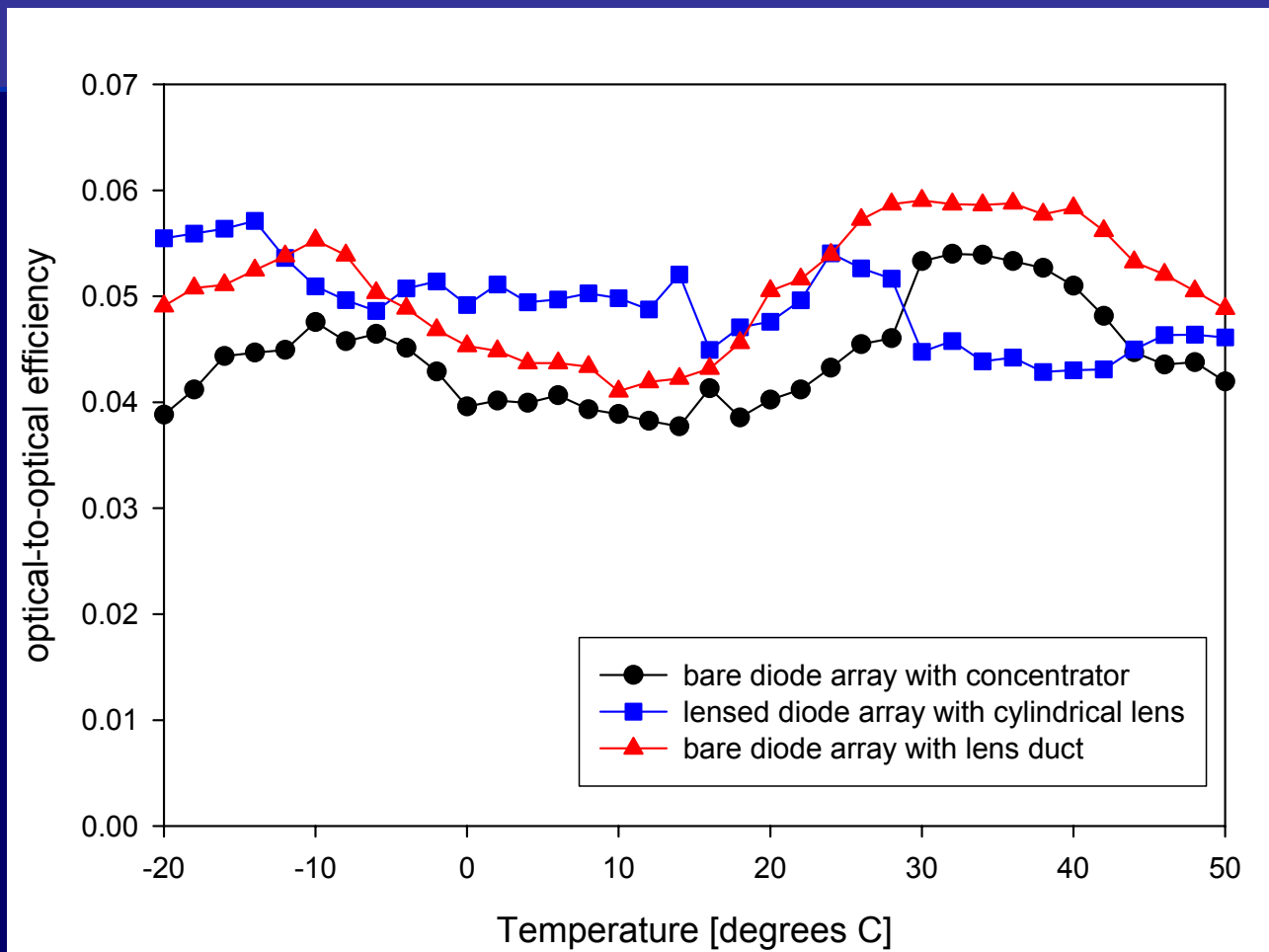
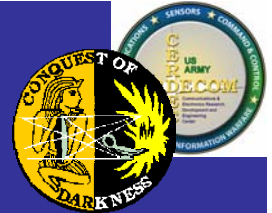


30°C



Temperature Testing

Optical to optical efficiency





Conclusions



- The next generation monoblock laser, a low-cost, compact, and rugged transmitter with application to eyesafe rangefinding and other targeting scenarios.
- Investigated several end-pumping schemes with application to the monoblock laser
- Experimentally compared the configurations over a 70°C temperature span from -20°C to 50°C
- Each of the tested end-pump configurations gave complete operation over the full temperature range.
- We have addressed the need for an eyesafe laser transmitter operating in the millijoule regime at tens of Hz repetition rate with optical to optical efficiency of 1-5%.